Desalination and Water Treatment
www.deswater.com

doi:10.5004/dwt.2019.24239

160 (2019) 308–315
August

Activated rice husk ash-supported silver nanoparticles as a novel adsorbent toward chloride removal

Trung Thanh Nguyen[a,*], Surapol Padungthon[b], Nhat Huy Nguyen[c]

[a]*Laboratory of Nanomaterial, An Giang University, VNU-HCM, 18 Ung Van Khiem St., Dong Xuyen Dist., Long Xuyen City, An Giang Prov., Vietnam, email: ntthanh@agu.edu.vn (T.T. Nguyen)*
[b]*Department of Environmental Engineering, Khon Kaen University, 123 Moo 16 Mittraphap Rd., Nai-Muang, Muang District, Khon Kaen 40002, Thailand, email: surapol.padungthon@gmail.com (S. Padungthon)*
[c]*Faculty of Environment and Natural Resources, Ho Chi Minh City University of Technology, VNU-HCM, 268 Ly Thuong Kiet St., Dist. 10, Ho Chi Minh City, Vietnam, email: nnhuy@hcmut.edu.vn (N.H. Nguyen)*

Received 9 September 2018; Accepted 8 April 2019

ABSTRACT

Chloride contamination of water from climate change and salty waste water is known as a serious issue of water and wastewater treatment. In this study, Ag/ARHA (activated rice husk ash) material was designed and fabricated as a novel adsorbent for chloride removal in aqueous solution. The deposition of Ag on ARHA material was done by a facile precipitation method using $AgNO_3$ as precursor and $NaBH_4$ as reductant. The material was then characterized by Fourier transform infrared spectroscopy, X-ray diffraction, transmission electron microscopy, and Brunauer–Emmett–Teller analyses. In chloride removal test, the Ag/ARHA adsorbent showed high chloride capacity of 7.9 mgCl^-/g Ag with good durability after at least ten cycles of adsorption–desorption. This high capacity could be due to the strong interaction between the ARHA support and Ag metal as well as the chemical adsorption of chloride onto silver nanoparticle surface on ARHA support with high surface area. Additionally, $H_2O_2$was proven as an effective solution for regeneration of the used Ag/ARHA adsorbent. Since the selectivity of Ag/ARHA for chloride removal was very high and seemly not affected by other anions, this novel adsorbent has a great potential for chloride contaminated water and wastewater treatment applications.

Keywords: Activated rice husk ash; Chloride removal; Silver nanoparticles; Water treatment

1. Introduction

The presence of chloride in water environment (e.g., surface water, underground water, and wastewater) as total dissolved solid is still one of the big challenge of water treatment processes. For example, low or lost efficiency of water treatment in Fenton system was observed by high concentration of chloride due to the reaction of hydroxyl radical and chloride ($OH^* + Cl^- \rightarrow ClOH^{*-}$; $k = 4.30 \times 10^9$ L·mol^{-1}·s^{-1}) [1,2]. Thus, wastewater with high chloride concentration must be diluted before further primary treatment although this is not a sustainable technology. On the other hand, the scarcity of clean water for human activities is being serious during the dry season at Mekong Delta (Vietnam) due to salt intrusion. Although many engineering approaches were proposed such as traditional water distillation, membrane [3], and anion resin exchange [4], the disadvantages of these technologies were observed for surface water and wastewater treatments with high salt concentration. These obstacles include high cost [3], complex operation and short lifetime of membrane (e.g. high suspension solid), and the low chloride selectivity for the anion resin exchange (e.g. sulfate, nitrate, and phosphate) [4].

For chloride removal by adsorption and ion exchange, some new materials have been developed for removal of chloride in water such as carbon xerogels [5], using modified hydrotalcite or hydrotalcite-like compounds [6,7],

*Corresponding author.

layered double hydroxides [8]. Since the synthesis of these new materials are complicated and costly, the ion exchange resin are still the most popular material which is studied and applied for chloride removal. Li et al. [9] studied on the modification of anion exchange to improve its ability, such as for removal of Tl (Thallium) and Cl^- in wastewater with high salinity. Liu et al. [10] combined anion exchange and ozone to remove chloride from wastewater of zinc production. Iakovleva et al. [11] employed limestones, iron sand, and waste from pulp and paper for adsorption of chloride and sulfate from mine process water. Dron and Dodi [4] used Amberlite® IRN 9766 (a macroporous resin) to compare the models for adsorption of anions, including chloride. Although many materials were studied and applied for chloride removal in aqueous phase, the issue for enhancing selective chloride adsorption have not still solved yet.

On the other hand, rice husk, a by-product of rice processing industry, is abundant in agricultural countries such as Vietnam and Thailand. Previously, rice husk is just simply dumped into the soil or water environment as a solid waste. Recently, rice husk is used as fuel in boiler, dryer, brick kiln and other combustion equipment and rice husk ash (as both bottom and collected fly ash) become a waste that need to be properly disposed. Several studies have been done on the management and utilization of rice husk ash [12–14]. Although the use of rice husk ash as silica source for nanomaterial fabrication and environmental application, there has been no work on the use of rice husk ash for chloride adsorption.

In this study, Ag/ARHA (activated rice husk ash) material was synthesized and applied as a novel adsorbent with high selectivity for chloride removal in solution. This suggests a new solution for chloride removal from surface water and wastewater or insecticide (i.e. chloramine chemicals) removal from treated surface water.

2. Materials and experiment

2.1. Chemicals and materials

Analytical grade HF (40 vol.%), $AgNO_3$, and standard chloride solution were purchased from Sigma Aldrich and Merck through chemical companies in Vietnam and used without further purification. Rice husk ash (RHA) material was collected from a furnace for brick production in An Giang Province, Vietnam.

2.2. Material synthesis

The novel support from RHA with high surface area was generated by a simple HF corrosion method reported in our previous work [15]. In a typical procedure, 20 mg of dried RHA was added into 80 mL of 10% (v/v) HF solution in plastic containers. After 30 min of stirring at ambient condition (i.e., 1 atm and room temperature), the activated RHA(ARHA) was collected after several times of washing with deionized (DI) water and centrifugation. The material was then dried in a vacuum oven at 80°C overnight.

Silver nanoparticles was deposited onto the surface of ARHA support by reducing silver ion with $NaBH_4$ reductant in aqueous solution. In a typical procedure, $NaBH_4$ was directly added into a mixture of ARHA and $AgNO_3$ solution under constant stirring. The reducing reaction of silver ion was carried out at room temperature for 30 min, followed by washing with DI water and centrifugation several times. The black powder obtained after drying in an oven at 100°C overnight was denoted as x%Ag/ARHA with x is the theoretical weight percentage of Ag (i.e. 5% and 10%).

2.3. Material characterizations

Wide angle X-ray diffraction (WAXRD) patterns were recorded on a D2 Phaser XRD 300 W diffractometer using CuKα radiation (λ = 1.5406 Å) with a step size of 0.05° and step time of 30 s. The morphology and particle size of ARHA and Ag/ARHA were evaluated using scanning electron microscopy (SEM) with energy-dispersive X-ray spectroscopy (EDS) and transmission electron microscopy (TEM) on a Philips Tecnai G^2 F20 TEM microscope operated at 40 kV. The specimens were prepared by ultrasonically suspending the materials in ethanol and the suspension was then applied to a copper grid and dried in an oven. Brunauer–Emmett–Teller (BET) surface area and pore size of the materials were determined from N_2 adsorption/desorption isotherms at 77 K using a sorptiometer (Porous Materials, BET-202A). Before BET measurement, the materials were degassed at 150°C for 4 h to completely remove residual water from the oxide meso-/micropores. Accordingly, the BET data correspond to the annealed samples. The Ag loading on the ARHA support was determined using inductively coupled plasma-atomic emission spectrometry (ICP-AES).

2.4. Chloride removal experiment

Aqueous chloride removal tests were performed at ambient conditions. In a typical experiment, 20 mg of Ag/ARHA powder was added into the 50 mL of 300 ppm NaCl solution. After chloride adsorption, the material was separated by centrifugation at 10.000 rpm for 10 min and the supernatant was collected for chloride analysis. Chloride concentration in the solution was determined by ionic chromatography method. The chloride adsorption capacity q (mg/g) of materials was calculated as following:

$$q = \frac{(C_o - C)}{m} \times 50 \quad (1)$$

where C_o and C are chloride concentrations in the solutions before and after adsorption (mg Cl^-/L) and m is amount of Ag in adsorbent (mg).

3. Results and discussion

3.1. Materials synthesis and characterizations

Figs. 1 and 2 display the FTIR and XRD results, respectively, of as-prepared and Ag-deposited ARHA materials. As seen in Fig. 1, FTIR patterns of ARHA material were characterized by oscillations of Si-O-Si (1100 cm^{-1}), C=C (1600 cm^{-1}), C=O (1730 cm^{-1}), and –OH (3450 cm^{-1}) [16]. Additionally, XRD patterns also showed that C and SiO_2 are the two main compositions of fresh ARHA material while AgCl

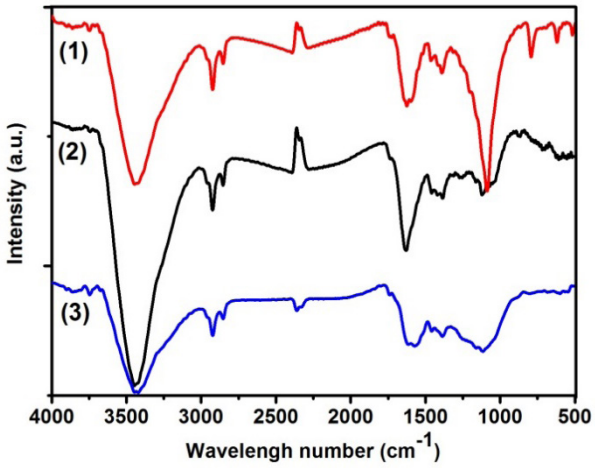

Fig. 1. FTIR patterns of (1) ARHA, (2) 5%Ag/ARHA, and (3) 5%Ag/ARHA (after chloride adsorption).

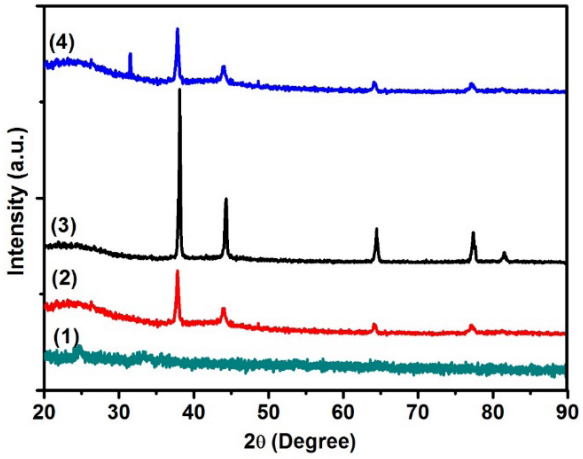

Fig. 2. XRD patterns of (1) ARHA, (2) 5%Ag/ARHA, (3) 10%Ag/ARHA, and (4) chloride saturated 5%Ag/ARHA materials.

peak was found for 5%Ag/ARHA after chloride adsorption (Fig. 2). Furthermore, amorphous structure was obtained for SiO_2 component in the ARHA support, which is similar to previous study [17]. After activated by HF, the obtained ARHA showed very high surface area of 416 m^2/g (Table 1), which was ca. 22 times higher than that of raw RHA (19 m^2/g). This much higher surface area would be attributed to the huge amount of pores observed in ARHA material (Fig. 3C) as compared to RHA (Fig. 3A). Notably, the EDS results showed that C/Si ratio significantly increased from 0.09 for RHA to 4.52 for ARHA samples (Figs. 3B and 3D). This proves the successful corrosion of HF chemical for silica composition in RHA [15], which made the porous structure of ARHA material.

The deposition of silver metal nanoparticles onto the surface of ARHA support was examined by FTIR (Fig. 1), XRD (Fig. 2), TEM (Fig. 4),and BET (Table 1) analysis. For FTIR result, the peak intensity for Si-O-Si oscillation at 1100 cm^{-1} [16] of Ag/ARHA was lower than that of ARHA support due to the covering of Ag nanoparticles on SiO_2 surface

Table 1
Surface area of materials

Sample	BET surface area (m^2/g)
RHA	19
ARHA	416
5%Ag/ARHA	408

sites. For XRD result, the peaks at 2θ of 38, 44, 64, 77, and 82° are known to be the characteristic peaks of silver nanoparticles [18,19]. TEM images in Fig. 4 also show that the silver nanoparticle size of 5%Ag/ARHA (actual Ag loading of 4.82 wt.% by ICP-AES) was less than 10 nm while that of 10%Ag/ARHA (actual loading of 9.91 wt.%) was greater than 12 nm, respectively. The smaller size of silver nanoparticles in 5%Ag/ARHA sample was consistent with XRD result (Fig. 2) because of its lower Ag loading. From Table 1, BET surface area of 5%Ag/ARHA (408 m^2/g)was slightly lower than that of ARHA. This is possibly due to the deposition and covering of Ag nanoparticles onto the surface and pores of ARHA material. Moreover, the surface area of silver is much lower than that of ARHA. As a result, the surface area of Ag/ARHA was slightly lower than that of ARHA.

3.2. Adsorption of chloride into Ag/ARHA nanomaterial

The chloride removal using Ag/ARHA adsorbent was investigated under various conditions of adsorption time, temperature, and pH value. Fig. 5 presents the effect of pH on the adsorption of chloride using 5%Ag/ARHA adsorbent. It can be concluded that pH from 5 to 8 is the optimum range for chloride adsorption. Additionally, the lower chloride adsorption capacities were observed in both conditions of acidic and basic environments, which can be due to the unfavorable charge on the silver surface and/or silver species for chloride adsorption under these conditions.

Fig. 6 illustrates the effects of adsorption time (Fig. 6A) and temperature (Fig. 6B) on the chloride adsorption. In Fig. 6A, a fast equilibrium was obtained after short adsorption time of around 20 min for Ag/ARHA materials, proving that it is a promising adsorbent for environmental applications. This can be attributed to the chemical adsorption and the strong interaction support metal (SISM) with charged silver surface[20,21]. As known, the SISM is created from the interaction between metal and support (e.g. oxide supports) which significantly contribute to the interfacial and transport phenomena as well as charge redistribution [22–25]. The SISM had three effects on the material, including electronic, geometric, and bifunctional effects [23]. Although further in-depth studies are required, it is possible that the SISM formed from Ag nanoparticles and silica (in ARHA) could change the electronic property of electron on the surface of Ag nanoparticles.

Additionally, Fig. 6A also shows that, while chloride adsorption was not observed for ARHA material, the chloride capacity of 5%Ag/ARHA adsorbent reached 7.9 mg Cl^-/gAg. It is noticeable that the surface area of 5%Ag/ARHA is smaller than that of ARHA, suggesting that Ag nanoparticles are the major adsorption sites for chloride adsorption while ARHA material plays a role as carrier or supporting

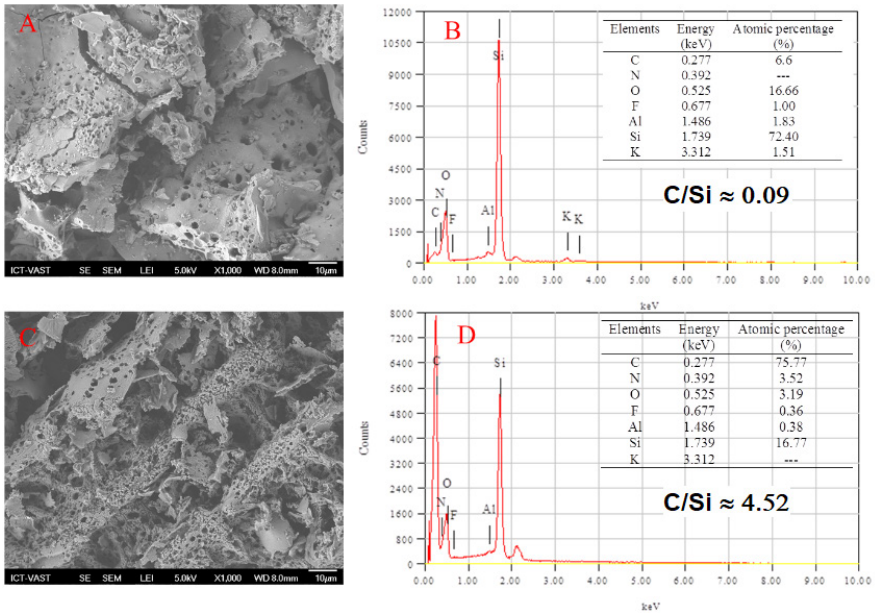

Fig. 3. SEM images and EDS results of RHA (A and B) and ARHA (C and D) materials, respectively.

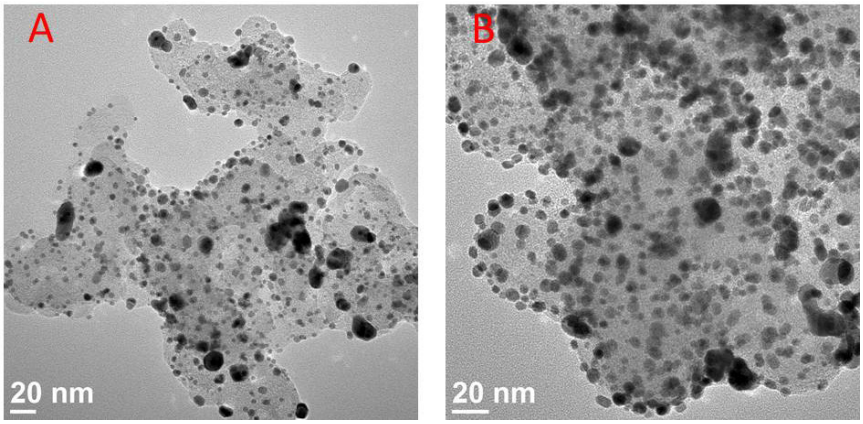

Fig. 4. TEM images of (A) 5%Ag/ARHA and (B) 10%Ag/ARHA materials.

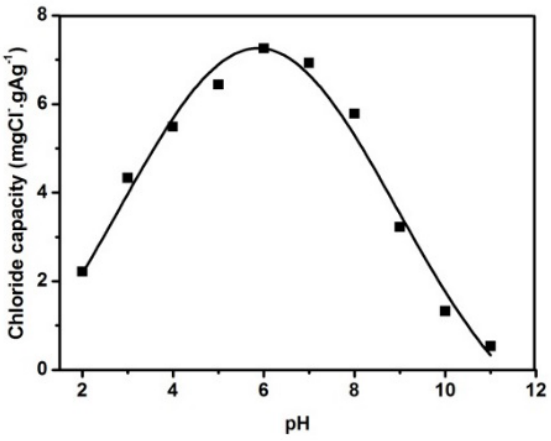

Fig. 5. Effect of pH on chloride adsorption using 5%Ag/ARHA adsorbent. (Condition: 60 min adsorption time, room temperature).

material. The temperature effect was investigated from 30 to 50°C, which is the temperature range of water and wastewater in practical applications. As observed in Fig. 6B, the chloride adsorption capacities using Ag/ARHA adsorbents increased with the increase of temperature while no effect was found for ARHA material. The linear relationship of temperature and adsorption capacity was obtained for 10%Ag/ARHA but non-linear relationship was found for 5%Ag/ARHA. This difference can be explained by the different adsorption kinetic between these two samples with different loadings and SISM [21,24,25]. For high Ag loading with large Ag nanoparticles, the decrease of SISM between Ag and ARHA (e.g. electronic property) lead to a decrease in chloride adsorption on the surface of silver nanoparticles (with the same Ag dose). Generally, this result confirms that the adsorption of chloride onto surface of silver nanoparticles is chemical adsorption.

Kinetic and thermodynamic study of adsorption is usually performed for better understanding the physico

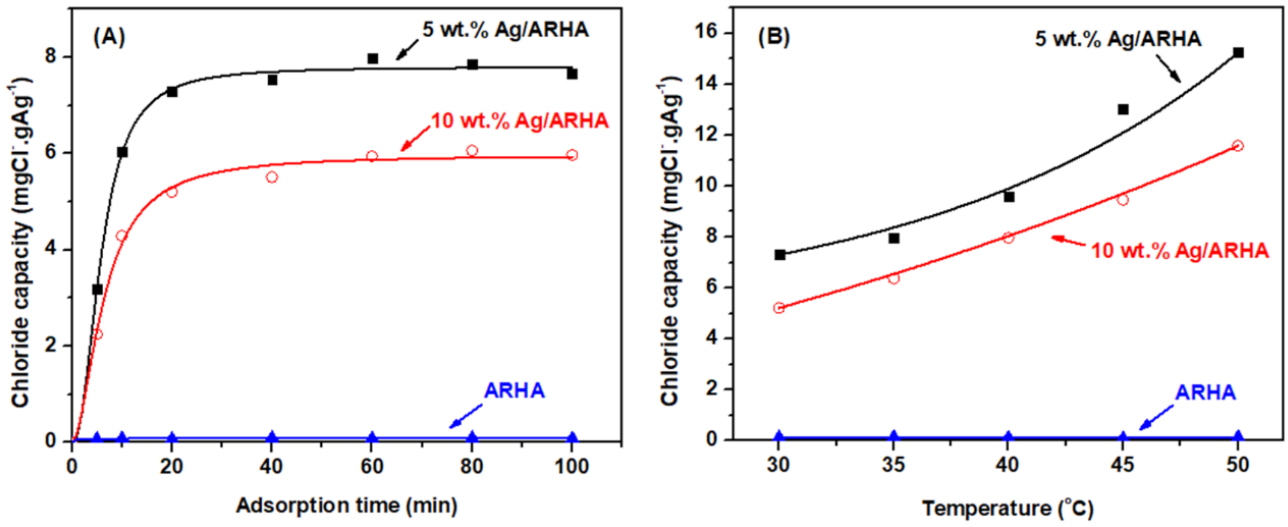

Fig. 6. Effects of (A) adsorption time and (B) temperature on chloride adsorption of ARHA, 5Ag/ARHA, and 10Ag/ARHA adsorbents. (Condition: pH 7, room temperature (Fig. 6A), 30 min adsorption time (Fig. 6B)).

-chemical properties of the adsorption as well as to find the suitable condition for high adsorption capacity. There are four kinetic models which are popular for describing the adsorption process, as followings.

Pseudo-first-order model:

$$\ln\left(Q_e - Q_t\right) = \ln Q_e - k_1 t \tag{2}$$

Modified-pseudo-first-order model:

$$\frac{Q_t}{Q_e} + \ln\frac{Q_t}{Q_e} + \ln\left(Q_e - Q_t\right) = \ln Q_e - K_1 t \tag{3}$$

Pseudo-second-order model:

$$\frac{t}{Q_t} = \frac{1}{k_2 Q_e^2} + \frac{t}{Q_e} \tag{4}$$

Intra-particle diffusion model:

$$Q_t = k_{ip} t^{0.5} \tag{5}$$

where Q_e (mg/g) and Q_t (mg/g) were adsorption capacity of material at equilibrium and time t (min), respectively. k_1 (min^{-1}), K_1 (min^{-1}), k_2 (g/mg·min), and k_{ip} (mg/g·min) were the rate constants of pseudo-first-order model, modified-pseudo-first-order model, pseudo-second-order model, and intra-particle diffusion model, respectively.

The kinetic study results for chloride adsorption using ARHA, 5%Ag/ARHA, and 10%Ag/ARHA are presented in Table 1. The suitability of a model was evaluated based on the R^2 (correlation coefficient), $Q_{e,cal}$, (capacity calculated from model), and $Q_{e,exp}$ (capacity obtained from experiment) values. In this study, the pseudo-second-order model with R^2 = 0.9918–0.9976 and $Q_{e,cal}$ = 0.0941–8.1900 mg/g is the most fitted model that can be used to describe the adsorption process of chloride on the material Ag/ARHA surface. This also implies that the adsorption rate was controlled by the chemical adsorption.

Thermodynamic study was also done for adsorption of chloride using 5%Ag/ARHA material. The temperature range was 30–50°C (303–323 K). Thermodynamic parameters and free energy change were calculated using following equations:

$$\ln K_d = \frac{\Delta S}{R} - \frac{\Delta H}{RT} \tag{6}$$

$$\Delta G = \Delta H - T\Delta S \tag{7}$$

where K_d is thermodynamic equilibrium constants. ΔH (kJ·mol^{-1}) and ΔS (J·mol^{-1}·K^{-1}) are calculated from plot of lnK_d and $1/T$ (Fig. 7). ΔG (kJ·mol^{-1}) is the free energy change.

The thermodynamic parameters are summarized in Table 3. The positive value of ΔH prove that adsorption of chloride on 5%Ag/ARHA is an endothermic process. At the same time, the positive value of ΔS indicates that the randomness of solid–liquid interface increases after adsorption, which implies the high affinity of 5%Ag/ARHA for chloride adsorption. Moreover, the lower value of ΔG at higher temperature showed that the adsorption is more feasible and spontaneous at lower temperature.

3.3. Stability test of Ag/ARHA adsorbent

The stability test result of 5%Ag/ARHA nanomaterial during 10 cycles of chloride adsorption–regeneration is presented in Fig. 8. It was found that the durability of the material strongly depended on the method of regeneration. In this study, the adsorbent was regenerated by dipping 20 mg of used Ag/ARHA in 20 mL solution of 3% (v/v) H_2O_2 or 0.5 M NaOH for 2 h. As seen in Fig. 8, the adsorption capacity of Ag/ARHA adsorbent was remarkably stable when reactivation with H_2O_2 solution. On the other hand, it drastically declined when using NaOH solution, proven that H_2O_2 is a more suitable solution for adsorbent reactivation.

The mechanism for adsorption of chloride ion and desorption by H_2O_2 is proposed in Fig. 9. Previous results

indicated that the chloride adsorption of silver nanoparticles followed chemical adsorption as verified by AgCl 2θ peak of 32° in XRD results (line 4 of Fig. 2) and was impacted under SISM due to the electronic change of Ag nanoparticles at the interfacial of Ag and ARHA [21–25]. As a result, the adsorption force of chloride onto silver nanoparticles surface is too strong, which would affect the desorption method for Ag/ARHA material. The desorption method using NaOH is based on the ion exchange between the adsorbed chloride on adsorbent surface (Cl^-_{ads}) and OH^-, so Cl^- ions on solid surface is hard to be completely replaced by OH^- group. On the other hand, reactivation using H_2O_2 is facilitated by chemical reactions (1) and (2), which effectively remove chloride from solid surface [26].

$$H_2O_2 + Cl^- + H_3O^+ \rightarrow HClO + 2H_2O \quad (8)$$

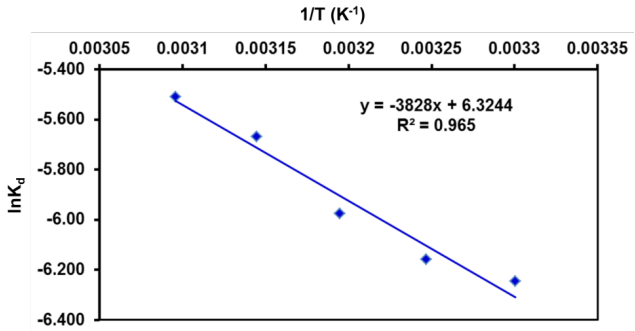

Fig. 7. Thermodynamic plot for adsorption of chloride by 5%Ag/ARHA material.

$$HClO + Cl^- + H_3O^+ \rightarrow Cl_2 + 2H_2O \quad (9)$$

3.4. Effect of co-existing anions

In natural environment, chloride contaminated water often contains several other anions such as SO_4^{2-}, NO_3^-, and PO_4^{3-}. The coexisting anions could compete with chloride anion for adsorption sites and, as a result, reduce chloride removal efficiency. Therefore, effect of these individual anions with different concentrations (i.e., 0, 50, 100, and 200 mg/L) on the chloride removal efficiency (300 mg/L) was carried out. As demonstrated in Fig. 10, all SO_4^{2-},

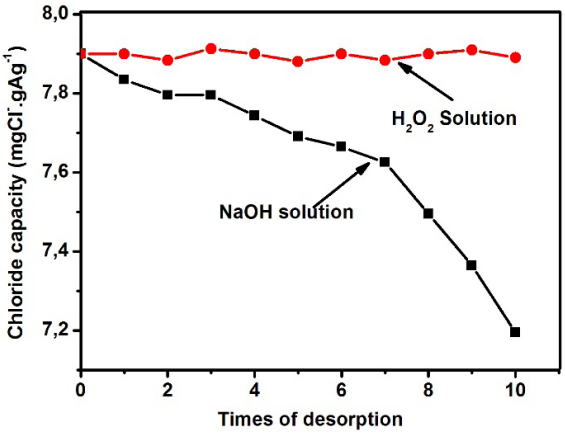

Fig. 8. Stability test for 5%Ag/ARHA adsorbent using NaOH and H_2O_2 solutions for regeneration.

Table 2
Parameters for different adsorption kinetics models

Model	Parameter	Adsorbent		
		ARHA	5%Ag/ARHA	10%Ag/ARHA
Pseudo-first-order model	$Q_{e,cal}$ (mg/g)	0.0241	1.9094	2.7053
	k_1 (min^{-1})	0.0059	0.0327	0.0405
	R^2	0.2251	0.4481	0.8369
Modified-pseudo-first-order model	$Q_{e,cal}$ (mg/g)	0.0519	3.7199	4.9774
	K_1 (min^{-1})	0.0048	0.0287	0.0357
	R^2	0.2130	0.4180	0.8340
Pseudo-second-order model	$Q_{e,cal}$ (mg/g)	0.0941	8.1900	6.4516
	k_2 ($g \cdot mg^{-1} \cdot min^{-1}$)	14.533	0.0292	0.0244
	R^2	0.9918	0.9961	0.9976
Intra-particle diffusion model	k_{ip} ($mg \cdot g^{-1} \cdot min^{-1/2}$)	0.0016	0.4569	0.3987
	R^2	0.3505	0.6167	0.7349

Table 3
Thermodynamic parameters of chloride adsorption on 5%Ag/ARHA

ΔH (kJ/mol)	ΔS (J/mol·K)	ΔG (kJ/mol)					R^2
		303 K	308 K	313 K	318 K	323 K	
31.828	52.581	15.896	15.633	15.370	15.107	14.844	0.9650

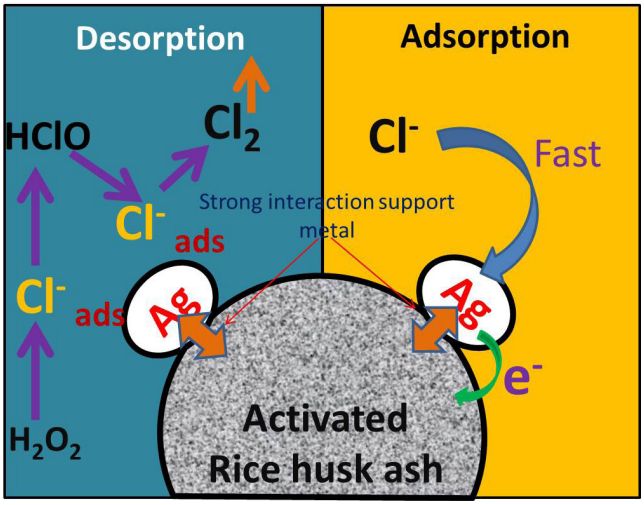

Fig. 9. Proposed mechanism for adsorption and desorption of chloride ion on Ag/ARHA surface.

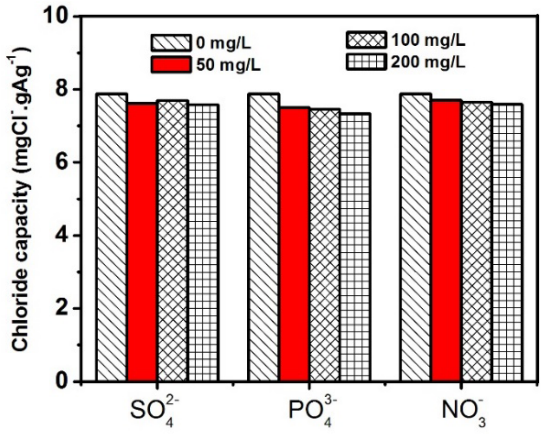

Fig. 10. Effect of co-existing anions on chloride adsorption by Ag/ARHA.

NO_3^-, and PO_4^{3-} anions had negative effect on the chloride removal by Ag/ARHA. However, these effects were not significant and Ag/ARHA material showed considerably high selectivity for chloride adsorption. As discussed previously, the adsorption function of Ag/ARHA was based on chemical adsorption. Therefore, other coexisting anions would not intensively affect chloride removal by Ag/ARHA material. This makes Ag/ARHA become a novel and unique material for chloride removal, which is potential for water and wastewater treatment in practical applications.

4. Conclusions

In summary, Ag/ARHA material was successfully synthesized and characterized with good dispersion of silver nanoparticles on the ARHA surface support. The Ag/ARHA material was proven as a novel adsorbent for aqueous chloride removal with high adsorption capacity and stability due to the strong interaction of support-metal and high surface area of ARHA support. The using of 3% (v/v) H_2O_2 solution was a preferable method for reactivation of used Ag/ARHA material after chloride adsorption. This study suggests that Ag/ARHA material has a great potential for water and wastewater treatment applications since it has extremely high selectivity for chloride removal. Future works should focus on the effect of environmental factors such as initial chloride concentration (and isotherms) and adsorption dosage and the application of Ag/ARHA for actual water samples.

Acknowledgments

The authors are grateful for financial support from An Giang University, Vietnam. The synchrotron research funding from Khon Kaen university, research program on development of appropriate technologies for coloring agent removal from textile dyeing, pulp & paper, and sugar industries for sustainable management, center of excellence on hazardous substance management (HSM), Chulalongkorn university, and research center for environmental and hazardous substance management (EHSM), Khon Kaen University.

References

[1] T.D.D. Oliveira, W.S. Martini, M.D.R. Santos, M.A.C. Matos, L.L.D. Rocha, Caffeine oxidation in water by Fenton and Fenton-like processes: effects of inorganic anions and ecotoxicological evaluation on aquatic organisms, J. Brazil. Chem. Soc., 26 (2015) 178–184.
[2] J. De Laat, T.G. Le, Effects of chloride ions on the iron(III)-catalyzed decomposition of hydrogen peroxide and on the efficiency of the Fenton-like oxidation process, Appl. Catal. B: Environ., 66 (2006) 137–146.
[3] M. Heiranian, A.B. Farimani, N.R. Aluru, Water desalination with a single-layer MoS_2 nanopore, Nature Commun., 6 (2015) 8616.
[4] J. Dron, A. Dodi, Comparison of adsorption equilibrium models for the study of Cl^-, NO_3^- and SO_4^{2-} removal from aqueous solutions by an anion exchange resin, J. Hazard. Mater., 190 (2011) 300–307.
[5] M.C. Zafra, P. Lavela, G. Rasines, C. Macías, J.L. Tirado, Effect of the resorcinol/catalyst ratio in the capacitive performance of carbon xerogels with potential use in sodium chloride removal from saline water, J. Solid State Electrochem., 18 (2014) 2847–2856.
[6] J. Hua, L. Lu, Chloride removal from wastewater by thermally treated hydrotalcite, Chinese J. Geochem., 25 (2006) 255–256.
[7] T. Kameda, T. Yoshioka, T. Hoshi, M. Uchida, A. Okuwaki, The removal of chloride from solutions with various cations using magnesium–aluminum oxide, Sep. Purif. Technol., 42 (2005) 25–29.
[8] F.L. Theiss, S.J. Couperthwaite, G.A. Ayoko, R.L. Frost, A review of the removal of anions and oxyanions of the halogen elements from aqueous solution by layered double hydroxides, J. Colloid Interface Sci., 417 (2014) 356–368.
[9] H. Li, Y. Chen, J. Long, D. Jiang, J. Liu, S. Li, J. Qi, P. Zhang, J. Wang, J. Gong, Q. Wu, D. Chen, Simultaneous removal of thallium and chloride from a highly saline industrial wastewater using modified anion exchange resins, J. Hazard. Mater., 333 (2017) 179–185.
[10] W. Liu, L. Lü, Y. Lu, X. Hu, B. Liang, Removal of chloride from simulated acidic wastewater in the zinc production, Chinese J. Chem. Eng., (2018).

[11] E. Iakovleva, E. Mäkilä, J. Salonen, M. Sitarz, M. Sillanpää, Industrial products and wastes as adsorbents for sulphate and chloride removal from synthetic alkaline solution and mine process water, Chem. Eng. J., 259 (2015) 364–371.
[12] R. Pode, Potential applications of rice husk ash waste from rice husk biomass power plant, Renew. Sustain. Energy Rev., 53 (2016) 1468–1485.
[13] J. Prasara-A, S.H. Gheewala, Sustainable utilization of rice husk ash from power plants: A review, J. Cleaner Prod., 167 (2017) 1020–1028.
[14] S. Kumar, P. Sangwan, R.M.V. Dhankhar, S. Bidra, Utilization of rice husk and their ash: A review, Res. J. Chem. Env. Sci., 1 (2013), 126–129.
[15] N.T. Thanh, A mine-bearing activated rice husk ash for CO_2 and H_2S gas removals from biogas, KKU Eng. J., 43 (2016) 396–398.
[16] D.M. Ibrahim, S.A. El-Hemaly, F.M. Abdel-Kerim, Study of rice-husk ash silica by infrared spectroscopy, Thermochim. Acta, 37 (1980) 307–314.
[17] M.H. Zhang, R. Lastra, V.M. Malhotra, Rice-husk ash paste and concrete: Some aspects of hydration and the microstructure of the interfacial zone between the aggregate and paste, Cem. Concr. Res., 26 (1996) 963–977.
[18] S. Nath, S. Kumar Ghosh, S. Praharaj, S. Panigrahi, S. Basu, T. Pal, Silver organosol: synthesis, characterisation and localised surface plasmon resonance study, New J. Chem., 29 (2005) 1527–1534.
[19] Y. Meng, A sustainable approach to fabricating Ag nanoparticles/PVA hybrid nanofiber and its catalytic activity, Nanomaterials, 5 (2015) 1124.
[20] T.-T. Nguyen, V.T.T. Ho, C.-J. Pan, J.-Y. Liu, H.-L. Chou, J. Rick, W.-N. Su, B.-J. Hwang, Synthesis of $Ti_{0.7}Mo_{0.3}O_2$ supported-Pt nanodendrites and their catalytic activity and stability for oxygen reduction reaction, Appl. Catal., B, 154–155 (2014) 183–189.
[21] M.-C. Tsai, T.-T. Nguyen, N.G. Akalework, C.-J. Pan, J. Rick, Y.-F. Liao, W.-N. Su, B.-J. Hwang, Interplay between molybdenum dopant and oxygen vacancies in a TiO_2 support enhances the oxygen reduction reaction, ACS Catalysis, 6 (2016) 6551–6559.
[22] J. Wang, C. An, M. Zhang, C. Qin, X. Ming, Q. Zhang, Photochemical conversion of AgCl nanocubes to hybrid AgCl–Ag nanoparticles with high activity and long-term stability towards photocatalytic degradation of organic dyes, Canad. J. Chem., 90 (2012) 858–864.
[23] C.G. Vayenas, S. Brosda, C. Pliangos, The double-layer approach to promotion, electrocatalysis, electrochemical promotion, and metal–support interactions, J. Catal., 216 (2003) 487–504.
[24] T. Ioannides, X.E. Verykios, Charge transfer in metal catalysts supported on doped TiO_2: A theoretical approach based on metal–semiconductor contact theory, J. Catal., 161 (1996) 560–569.
[25] C.-J. Pan, M.-C. Tsai, W.-N. Su, J. Rick, N.G. Akalework, A.K. Agegnehu, S.-Y. Cheng, B.-J. Hwang, Tuning/exploiting strong metal-support interaction (SMSI) in heterogeneous catalysis, J. Taiwan Inst. Chem. E., 74 (2017) 154–186.
[26] J.K. Gaca, M. Mroz, The effect of chloride ions on alkylbenzenesulfonate degradation in the Fenton reagent, Polish J. Environ. Stud., 14 (2004) 23–27.